

Viaduct seismic response under spatial variable ground motion considering site conditions

Rachid Derbal^{*1,3}, Nassima Benmansour¹, Mustapha Djafour¹,
Mohammed Matallah¹ and Salvador Ivorra²

¹RISk Assessment & Management Laboratory (RISAM), University of Tlemcen, Po Box 230, Tlemcen, Algeria

²Department of Civil Engineering, University of Alicante, San Vicente del Raspeig, Apartado 99, 03080, Spain

³Department of Civil Engineering, Ctr. Univ. Ain Temouchent, Po. Box 284, Ain Temouchent, Algeria

(Received July 3, 2019, Revised September 7, 2019, Accepted October 24, 2019)

Abstract. The evaluation of the seismic hazard for a given site is to estimate the seismic ground motion at the surface. This is the result of the combination of the action of the seismic source, which generates seismic waves, the propagation of these waves between the source and the site, and site local conditions. The aim of this work is to evaluate the sensitivity of dynamic response of extended structures to spatial variable ground motions (SVGM). All factors of spatial variability of ground motion are considered, especially local site effect. In this paper, a method is presented to simulate spatially varying earthquake ground motions. The scheme for generating spatially varying ground motions is established for spatial locations on the ground surface with varying site conditions. In this proposed method, two steps are necessary. Firstly, the base rock motions are assumed to have the same intensity and are modelled with a filtered Tajimi-Kanai power spectral density function. An empirical coherency loss model is used to define spatial variable seismic ground motions at the base rock. In the second step, power spectral density function of ground motion on surface is derived by considering site amplification effect based on the one dimensional seismic wave propagation theory. Several dynamics analysis of a curved viaduct to various cases of spatially varying seismic ground motions are performed. For comparison, responses to uniform ground motion, to spatial ground motions without considering local site effect, to spatial ground motions with considering coherency loss, phase delay and local site effects are also calculated. The results showed that the generated seismic signals are strongly conditioned by the local site effect. In the same sense, the dynamic response of the viaduct is very sensitive of the variation of local geological conditions of the site. The effect of neglecting local site effect in dynamic analysis gives rise to a significant underestimation of the seismic demand of the structure.

Keywords: ground motion; spatial variability; simulation; wave propagation; coherency loss; local geological site effect

1. Introduction

For extended structures, such as bridges, seismic ground motions at different supports are inevitably not the same in terms of amplitude and phase. This is the result of seismic wave propagation and local site geological conditions. During an earthquake, spatial variation of ground motions are caused by coherency loss, wave passage and local site effects (Harichandran and Vanmarcke 1986, Der Kiureghian 1996).

Past investigations indicate that the effect of spatial variation of seismic motions on the structural responses cannot be neglected, and can be, in some cases, detrimental (Zerva 2009, Konakli and Der Kiureghian 2012). Most of these studies are based on spatial ground motion coherency loss functions and time delay. The site under consideration is assumed to be uniform and homogeneous.

In earthquake resistant design of multiple supports structures, properly define seismic ground motions is

fundamental for a reliable analysis of structural responses. For this purpose, the seismic ground motion must considering earthquake spatial variability in terms of loss coherency effect, wave passage effect and, in particular, local site effect (Derbal *et al.* 2018, Derbal *et al.* 2017, Zhang *et al.* 2013, Adanur *et al.* 2016, Yao *et al.* 2018, Shiravand and Parvanehro 2019).

Besides ground motion time histories, ground motion response spectrum and power spectral density function are the most commonly used parameters to define seismic load of a structure. Many ground motion power spectral density functions have been developed by different researchers, such as the Tajimi-Kanai power spectral model (Tajimi 1960) and the Clough-Penzien model (Clough and Penzien 1993). Both of them were proposed by assuming the base rock excitation is a white noise random process, and the surface ground motion is estimated by calculating the responses of a single soil layer to the white noise excitation (Bi *et al.* 2010).

It should be noted that considering site to be uniform and homogeneous, will lead to inaccurate ground motion representation in case of a canyon site (Bi *et al.* 2010, Bi and Hao 2012). At a canyon site, the spatial variable ground motions at base rock can still be assumed to have the same power spectral density, but on ground surface, the ground

*Corresponding author, Ph.D. Student

E-mail: r.derbal@yahoo.com;

rachid.derbal@cuniv-aintemouchent.dz

motion power spectral densities will be very different owing to seismic wave propagation through different wave paths that cause different site amplifications. Uniform ground motion power spectral density assumption in such situation may lead to erroneous the estimation of structural responses (Bi *et al.* 2010).

Many researchers have investigated the spatial varying seismic ground motion by considering local site effect. Bi *et al.* (2010), have proposed an approach where the spatial ground motions are modelled by considering that the base rock motions have the same intensity. A filtered Tajimi-Kanai power spectral density function and an empirical spatial ground motion coherency loss function are used to define seismic ground motion. Based on the one dimensional seismic wave propagation theory, power spectral density function of ground motion on surface is derived by considering the site amplification effect. A Discussion on the ground motion spatial variation and site amplification effects on structural responses are made. Bi *et al.* (2010) conclude that neglecting local site conditions on the spatial ground motion effects in structural analysis can lead to inaccurate estimation of dynamics responses.

Konakli and Der Kiureghian (2012) presented a simulation method of the spatial variable seismic ground motions incorporating the effects of incoherence, wave passage, and differential site response. They proposed two approaches. The first is the conditional simulation where the motions are consistent with the power spectral densities of a segmented recorded motion and are characterized by uniform variability at all locations. They affirmed that uniform variability in the array of ground motions is essential when synthetic motions are used for statistical analysis of the response of multiply-supported structures. While for the second simulation, the ground motions are conditioned on the segmented record itself and exhibit increasing variance with distance from the site of the observation. An example simulated motions are presented for an existing bridge model. The site effect is modeled using two ways. At the first, each soil-column is idealizing as a single degree of freedom oscillator. Then, they use the theory of vertical wave propagation in a single soil layer over bedrock. The proposed method was validated by comparing statistical characteristics of the synthetic motions with target theoretical models.

It should also be noted that often, for reasons of unavailability of seismic recordings in a region, several researchers resort to synthetic accelerograms (Beneldjouzi *et al.* 2017).

Based on the theory of wave propagation developed by Wolf (1985), Bi and Hao (2012) have developed an approach for generating asynchronous seismic ground motions considering local site effects. The motion at the rock base is assumed to be composed of SH wave (off-plan) or the combination of P and SV waves with an incident angle given. The generated seismic ground motions are compatible with the spectral density functions of target response spectra. It was conclude that the proposed approach leads to a more realistic modeling of the asynchronous seismic ground motions in sites with different characteristics compared to the assumption of same intensity of ground motion.

Using the model developed by Der Kiureghian (1996), Dumanoglu and Soyluk (2003) analyzed responses of a long span structure to spatially varying ground motions with site effect. It was concluded that although it was difficult to draw general conclusions because of the limited analyses performed, it was clear that ground motion spatial variation and site effects significantly affect the structural responses; considering different site effects at multiple supports generated larger structural responses; the more significant was the difference between the site conditions at the multiple supports, the larger was the structural responses. It was conclude that the site effects significantly affect structural responses.

It is know that seismic codes classify the foundation soil into several types giving them, predefined characteristics principally in terms of shear wave propagation velocity. Consequently, the characteristics of the real ground are converted to be equivalent as close as possible to a ground type defined by the seismic codes. Based on this principle, a spatially variable seismic ground motion generation model was developed taking into account the site effect by considering a single layer of soil.

Most recent studies have shown that the local site conditions should not be neglected when interpreting the spatial variability of seismic ground motion (Derbal *et al.* 2018, Derbal *et al.* 2017, Zhang *et al.* 2013, Yao *et al.* 2018, Shiravand and Parvanehro 2019). Consequently, the model proposed in this study takes into account all effects of spatial variability of ground motion, in particular the local site effect.

The aim of this study to quantify the influence of the site effect considering a spatial variability of seismic ground motion on the dynamic response of a railway viaduct. Several simulation of seismic spatial ground motion are made for each support. Dynamics responses to uniform ground motion and to spatial ground motion with and without considering site effect are calculated and compared. A discussion on the ground motion spatial variation and local soil site amplification effects on structural dynamics responses is made.

However, when considering SVGM, FE (Finite Element) dynamic analysis is generally performed using the displacement time histories as an input. In other words, the displacement time histories need to be evaluated from the spatially variable simulated accelerations. But experiences show that direct integration of the acceleration data often causes unrealistic drifts in the derived velocity and displacement. A correction scheme must be used to ensure compatibility between simulated accelerations, velocities and displacements time histories. In the present study, the simulation model of spatial ground motion model described by Benmansour *et al.* (2012) is used (Benmansour 2013). This model was developed to automatically derive the compatible displacement signals from spatially variable simulated accelerations.

2. Geometry of the railway viaduct

The railway viaduct is a part of the new high-speed line, situated in the north west of Algeria. Its typology is a

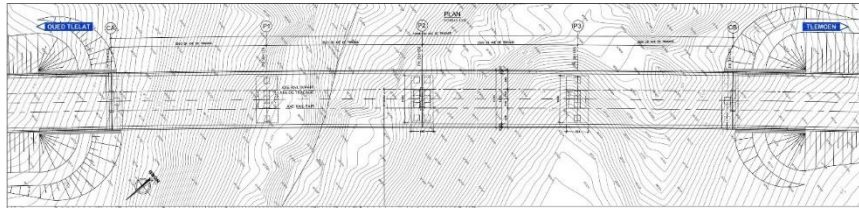


Fig. 1 Plan view of a viaduct

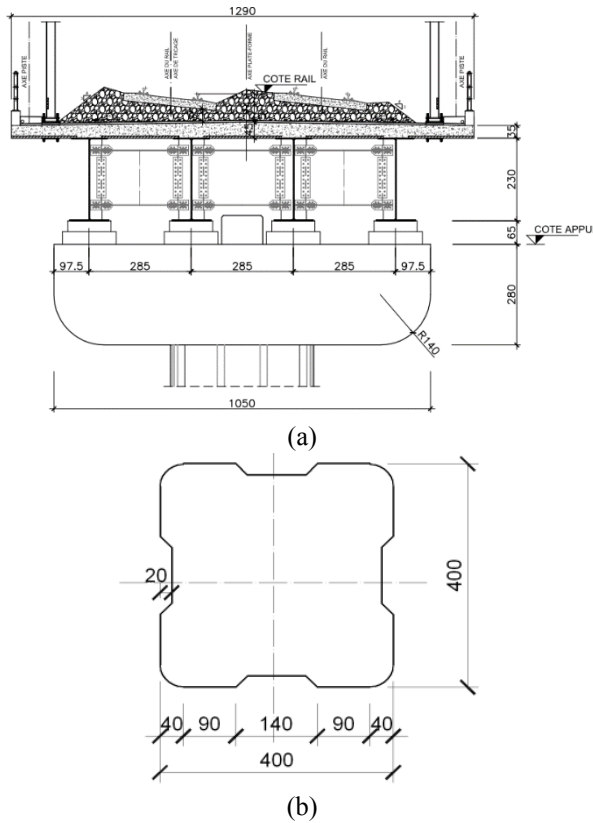


Fig. 2 Structural elements sections (in cm) (a) section of the deck; (b) Piers section

continuous deck with four spans of 35 m length (see Fig. 1), composed of steel beams with a height of 2.30 m supporting a concrete slab with average thickness of 0.40 m, resting on stacks of solid section (see Fig. 2(a)). The viaduct is curved with a total length of 140 m and a radius of curvature of 5000 m. It is a viaduct with two independent decks and three piles with height varies between 11.90 m and 17.90 m. The piers have a section of $4 \times 4 \text{ m}^2$. The detailed dimensions of this section are given in Fig. 2(b).

The dead loads supported by the deck are computed and given by Table 1. The compressive strength selected for the dynamic analysis of the viaduct structure is 35 MPa for piles and 30 MPa for the deck slab.

3. Viaduct finite element model

In order to perform a dynamic analysis of the viaduct, a 3D finite element model has been realized using a finite element code (see Fig. 3). The deck composed by steel beams and a concrete slab is idealized by shell elements

Table 1 Dead loads on the deck

Loads	Value (KN/ml)
Borders	3.75
Sidewalks	5.76
Rail UIC 60	2.40
Travres	9.60
Ballast	114.70
Waterproofing	17.05

Table 2 Periods and frequency of eigen modes of vibration

Mode	Mode 1	Mode 2	Mode 3	Mode 4
Period (s)	0.7299	0.6825	0.4529	0.4188

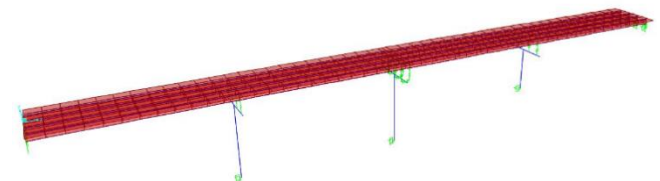


Fig. 3 Viaduct 3D finite element model

supported by linear elements. The connection between steel beams and the cap beams upside of piles is assumed rigid and it is modeled by fixed link elements. All dynamic analysis were performed in assumption of a 5% damping coefficient.

The first two eigen modes of vibration designate a transverse displacement along the Y axis. This is mainly due to the fact that the most vulnerable seismic action is in this direction.

4. Generation of spatially variable ground motions

4.1 Site configuration model

The site foundation is modeled in single layer soil with various characteristics at each support. Fig. 5 illustrates this model, in which i, j, k, l and m are the supports on ground surface. The corresponding points at the base rock are i', j', k', l' and m' respectively.

Table 3 gives the soil parameters where ρ_x , v_x , ξ_x and h_x ($x = 1, \dots, 5$) are densities, shear wave velocities, damping ratios and depths of the soil under support, respectively. The corresponding parameters on the base rock are $\rho_R = 30 \text{ KN/m}^3$, $v_R = 1500 \text{ m/s}$ and $\xi_R = 5\%$ (Bi and Hao 2012). Fig. 5 shows longitudinal view of a bridge crossing a canyon with variable site.

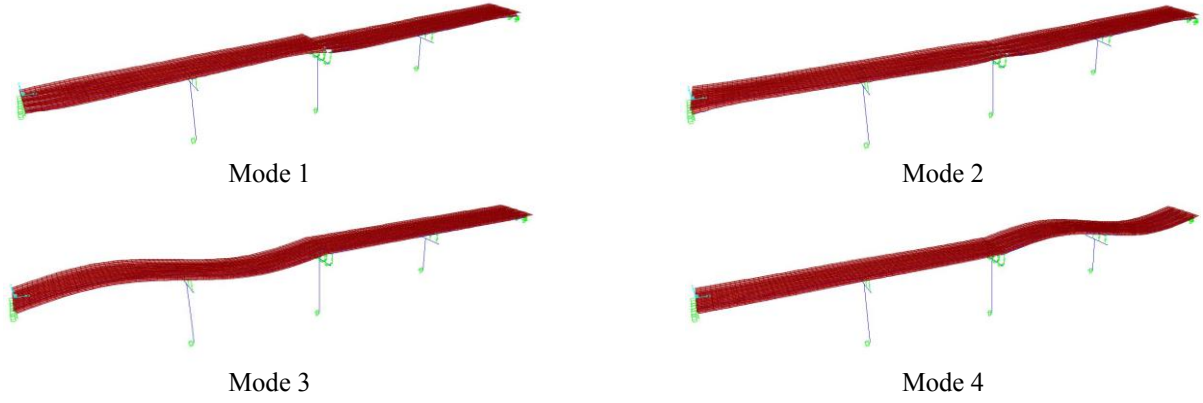


Fig. 4 Deformed shapes of the four modes of vibration

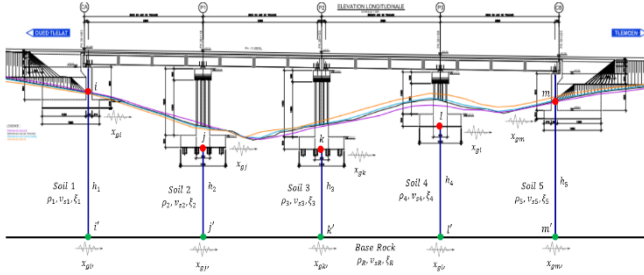


Fig. 5 Longitudinal view of viaduct crossing a canyon site

4.2 Base rock motion model

As assumption, the seismic ground motion at points i' , j' , k' , l' and m' which are on the base rock (see Fig. 5) have the same intensity in term of power spectral density. The filtered Tajimi-Kanai power spectral density function is used to define power spectral density at the base rock (Der Kiureghian 1996, Zerva 2009).

$$S_g(\omega) = |H_p(\omega)|^2 S_0(\omega) \quad (1)$$

$$|H_p(\omega)|^2 = \frac{\omega^4}{(\omega_f^2 - \omega^2)^2 + (2\omega_f\omega\xi_f)^2} \quad (2)$$

$$S_0(\omega) = \frac{\omega_g^4 + 4\xi_g^2\omega_g^2\omega^2}{(\omega_g^2 - \omega^2)^2 + 4\xi_g^2\omega_g^2\omega^2} \Gamma \quad (3)$$

In which $|H_p(\omega)|^2$ is a high pass filter (Bi *et al.* 2010), $S_0(\omega)$ is the Tajimi-Kanai power spectral density function (Tajimi 1960), ω_g and ξ_g are the central frequency and damping ratio of the Tajimi-Kanai power spectral density function, Γ is a scaling factor depending on the ground motion intensity, and ω_f and ξ_f are the central frequency and damping ratio of the high pass filter.

In this study, it is assumed that $\omega_f = 0.25 \times 2\pi\text{Hz}$, $\xi_f = 0.6$, $\omega_g = 5 \times 2\pi\text{Hz}$ and $\xi_g = 0.6$ (Bi *et al.* 2010). Assuming a ground acceleration of duration $T = 20\text{ s}$ and peak ground acceleration value $\text{PGA} = 0.5g$.

$\Gamma = 0.022\text{ m}^2/\text{s}^3$ is estimated in this study according to the standard random vibration approach described by Kreiughian (Der Kiureghian 1996, Bi *et al.* 2010).

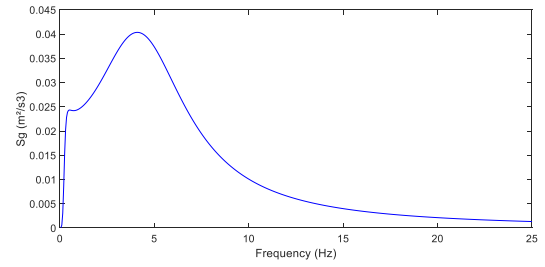


Fig. 6 Filtered ground motion power spectral density function on the base rock (in acceleration)

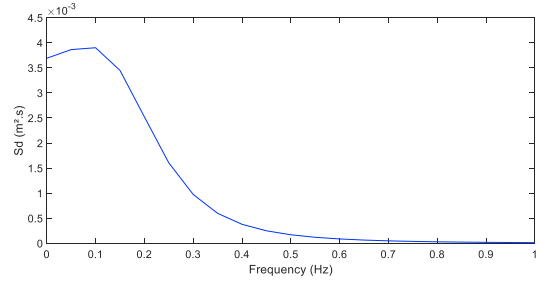


Fig. 7 Filtered ground motion power spectral density function on the base rock (in displacement)

Figs. 6 and 7 show the power spectral density of the base rock acceleration and displacement respectively.

4.3 Coherency loss model

Seismic ground round motions at two distant points can vary significantly from each other, because the propagating seismic waves have a different arrival time at these locations, and the geological medium in the wave path can affect the characteristics of the propagating waves (Der Kiureghian 1996, Zerva 2009, Konakli and Der Kiureghian 2012).

The coherency loss function is generally complex. In the frequency domain, this function describes the correlation between two seismic ground motion time histories in terms of amplitudes and phase angles. This function has the following form (Der Kiureghian 1996, Bi and Hao 2012).

$$\gamma_{jk}(\omega) = \frac{S_{jk}(\omega)}{\sqrt{S_{jj}(\omega) \cdot S_{kk}(\omega)}} \quad (4)$$

Table 3 Parameters of soil foundation

Soil 1		Soil 2		Soil 3		Soil 4		Soil 5	
ρ_1 (KN/m ³)	v_1 (m/s)	ρ_2 (KN/m ³)	v_2 (m/s)	ρ_3 (KN/m ³)	v_3 (m/s)	ρ_4 (KN/m ³)	v_4 (m/s)	ρ_5 (KN/m ³)	v_5 (m/s)
2000	450	1500	250	1500	300	1400	230	1800	350
ξ_1	$h_1(m)$	ξ_2	$h_2(m)$	ξ_3	$h_3(m)$	ξ_4	$h_4(m)$	ξ_5	$h_5(m)$
5%	56	5%	30	5%	29	5%	37	5%	54

Where:

ω is the circular frequency.

$S_{jj}(\omega)$, $S_{kk}(\omega)$ are the power spectral density functions of the time histories $g_j(t)$ and $g_k(t)$, respectively.

$S_{jk}(\omega)$ is the cross-power spectral density of the time histories $g_j(t)$ and $g_k(t)$.

This coherency loss function can be written as (Der Kiureghian 1996)

$$\gamma_{jk}(\omega) = |\gamma_{jk}(\omega)| \exp\left(-i \frac{\omega \cdot d_{jk}}{v_a}\right) \quad (5)$$

Where :

d_{jk} is the projected horizontal distance along the direction of propagation of the waves, which is from station j to station k .

v_a is the surface apparent velocity of waves, considered as constant over the frequency range of the wave.

In the numerical simulation of spatially varying ground motions usually empirical coherency loss functions are applied (Bi and Hao 2012). In the present paper, the Sobczyk model (Bi *et al.* 2010) is selected to describe the coherency loss between the ground motions at points i' and j' ($i' \neq j'$) at the base rock

$$\gamma_{j'k'}(\omega) = \exp(-\beta \cdot d_{j'k'}) \exp\left(-\alpha(\omega) \sqrt{d_{j'k'}} \left(\frac{\omega}{2\pi}\right)^2\right) \exp\left(-i \frac{\omega \cdot d_{j'k'}}{v_a}\right) \quad (6)$$

Where:

$d_{ij'}$ is the distance between the points j' and k' located at the base rock.

α is the incident angle of the incoming wave to the site, and is assumed to be $\pi/3$.

β is a coefficient which reflects the level of coherency loss, $\beta = 5 \cdot 10^{-4}$ (Bi *et al.* 2010).

$v_a = 1768$ m/s is at the base rock, according to the base rock property and the specified incident angle (Bi *et al.* 2010).

4.4 Spatial seismic ground motion model

Spatial earthquake ground motions on the base rock are assumed as stationary stochastic processes, with zero mean values, i.e., gaussian process, and having the same Tajimi-kanai power spectral density function (Deodatis 1996). The cross power spectral density function of ground motions at n locations in a site can be written as

$$S(i\omega) = \begin{bmatrix} S_{11}(\omega) & S_{12}(i\omega) & \dots & S_{1n}(i\omega) \\ S_{11}(i\omega) & S_{22}(\omega) & \dots & S_{2n}(i\omega) \\ \dots & \dots & \dots & \dots \\ S_{n1}(i\omega) & S_{n2}(i\omega) & \dots & S_{nn}(\omega) \end{bmatrix} \quad (7)$$

Using the definition of the coherence function cited above in Eq. (6), the cross power spectral density functions are written as follows (Bi *et al.* 2010, Bi and Hao 2012)

$$S_{jk}(\omega) = \sqrt{S_{jj}(\omega) \cdot S_{kk}(\omega)} \cdot \gamma_{jk}(\omega) \quad (8)$$

The matrix $S_{jk}(i\omega)$ is Hermitian and positive definite. So, it can be decomposed into the multiplication of a complex lower triangular matrix $L(i\omega)$ and its Hermitian $L^H(i\omega)$ as

$$S_{jk}(i\omega) = L_{jk}(i\omega) \cdot L_{jk}^H(i\omega) \quad (9)$$

The decomposition can be performed using the Cholesky's method. The lower triangular matrix $L_{jk}(i\omega)$ has the following form

$$L_{jk}(i\omega) = \begin{bmatrix} L_{11}(\omega) & L_{12}(i\omega) & \dots & L_{1n}(i\omega) \\ L_{11}(i\omega) & L_{22}(\omega) & \dots & L_{2n}(i\omega) \\ \dots & \dots & \dots & \dots \\ L_{n1}(i\omega) & L_{n2}(i\omega) & \dots & L_{nn}(\omega) \end{bmatrix} \quad (10)$$

The elements of $L_{jk}(i\omega)$ can be written in polar form as

$$L_{jk}(i\omega) = |L_{jk}(\omega)| \cdot \exp(i\theta_{jk}(\omega)) \quad j > k \quad (11)$$

Where

$$\theta_{jk}(\omega) = \tan^{-1} \left(\frac{\text{Im}[L_{jk}(\omega)]}{\text{Re}[L_{jk}(\omega)]} \right) \quad (12)$$

Using Eq. (10) and Eq. (11) the stationary stochastic vector process $g_j(t)$; $j = 1, 2, \dots, n$. can be simulated by the following series as $N \rightarrow \infty$ (Benmansour 2013, Miao *et al.* 2018)

$$g_j(t) = 2 \sum_{m=1}^n \sum_{l=1}^N |L_{jm}(\omega)| \cdot \sqrt{\Delta\omega} \cdot \cos(\omega_l t - \theta_{jm}(\omega_l) + \phi_{ml}) \quad (13)$$

Where

$$\omega_l = l\Delta\omega \quad l = 1, 2, \dots, N \quad (14)$$

$$\Delta\omega = \omega_u / N \quad (15)$$

N : represents the number of the frequency step $\Delta\omega$ needed to reach the upper cut-off frequency ω_u .

The $\{\phi_{ml}\}; m = 1, 2, \dots, n; l = 1, 2, \dots, N$ appearing in Eq. (13) are n sequences of independent random phase angles distributed uniformly over the interval $[0, 2\pi]$.

Note that the developed simulation approach of seismic spatial ground motion gives directly a stationary time history series $g_j(t)$ in terms of acceleration, velocity and displacement.

In this study, the non-stationary temporal variation of the simulated ground motions is expressed by multiplying the simulated stationary time histories by the Jennings envelope function (Jennings *et al.* 1968), as

$$f_j(t) = \zeta(t) \cdot g_j(t) \quad j = 1, 2, \dots, n \quad (16)$$

The Jennings envelope function has the following form

$$\zeta(t) = \begin{cases} (t/t_0)^2 & 0 \leq t \leq t_0 \\ 1 & t_0 < t \leq t_n \\ \exp[-0.155 \cdot (t - t_n)] & t_n < t \leq T \end{cases} \quad (17)$$

With $t_0 = 2$ s and $t_n = 10$ s.

For site amplification, we use the seismic wave propagation theory presented by Safak (1995), the transfer function for shear wave propagation in a horizontal layer of soil is given by

$$H_j(i\omega) = \frac{U_j(i\omega)}{U_j(i\omega)} \quad (18)$$

$$H_j(i\omega) = \frac{(1 + r_j - i\xi_j) \exp(-i\omega\tau_j(1 - 2i\xi_j))}{1 + (r_j - i\xi_j) \exp(-2i\omega\tau_j(1 - 2i\xi_j))} \quad (19)$$

Where:

$U_j(i\omega)$ and $U_j'(i\omega)$ is the Fourier transform of the $u_j(t)$ and $u_j'(t)$

ξ_j is the damping ratio accounting for energy dissipation owing to seismic wave propagation, $\xi_j = 1/4Q$ and Q is the quality factor.

τ_j is the wave propagation time from point j' to j with $\tau_j = h_j/v_j$

r_j is the reflection coefficient for up-going waves given by the equation:

$$r_j = \frac{\rho_R v_R - \rho_j v_j}{\rho_R v_R + \rho_j v_j} \quad (20)$$

The cross power spectral density function at point j and between point j and k has the following form

$$S_{jj}(\omega) = |H_j(i\omega)|^2 S_g(\omega) \quad (21)$$

$$S_{jk}(\omega) = H_j(i\omega) H_k^*(i\omega) S_{j'k'}(\omega) \quad (22)$$

with $j \neq k$ and $j' \neq k'$

The index "*" represents the complex conjugate.

It should be noted that the transfer function expressed in this study is derived for the case with a single layer of soil. The corresponding transfer functions for the five viaduct supports are illustrated in Fig. 8. This figure compares the transfer functions at surface points of viaduct with different

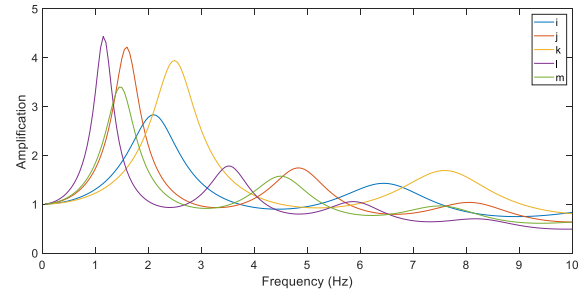


Fig. 8 Site effect on ground motion spatial variations at supports

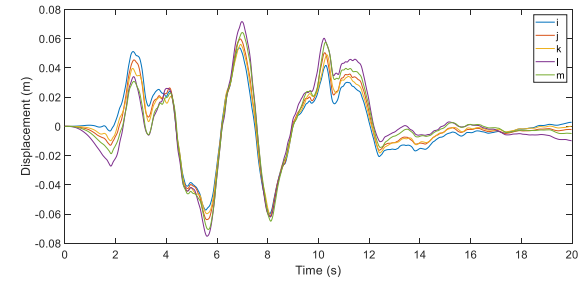


Fig. 9 Displacements generated considering all factors of spatial ground motion

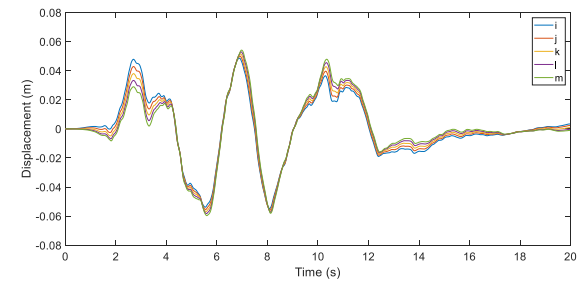


Fig. 10 Displacements generated without considering local site effects

soil types and thickness of layer. It indicates that the dominant frequency of a soil is dependent on its thickness, stiffness and density.

5. Application and discussion

5.1 Spatial seismic ground motion generated

The proposed spatial seismic ground motion model, described above in paragraph 4.4, is performed using code program. The generated spatial ground motions are calculated on the basis of the mean of one hundred simulations (Zerva 2009). From these simulations, we can have the spatial seismic ground motion as accelerations, velocity or displacements.

Figs. 9 and 10 gives the evolution of generated time history displacements in four cases: i) spatial seismic ground motion considering all factors of spatial ground motion, ii) spatial seismic ground motion without considering local site effect, iii) spatial seismic ground motion with considering only local site effect and iv)

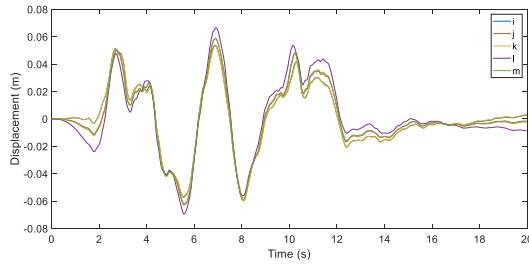


Fig. 11 Displacements generated with considering only local site effect

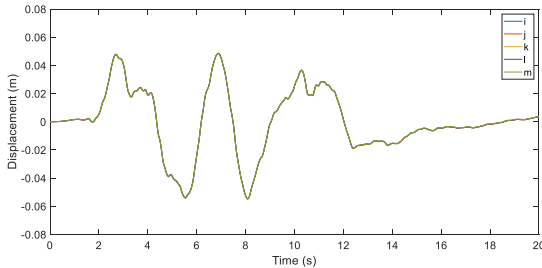


Fig. 12 Displacements generated in case of uniform seismic ground motion

uniform seismic ground motion.

Spatially correlated and non-stationary ground surface ground motions are produced on ground surface at points i , j , k , l and m for the case of spatial seismic ground motions considering all factors of earthquake spatial variability. Spatial seismic ground motion as displacements are shown in Figs. 9 to 12.

In Fig. 9, we observe that the generated displacements of the first case i.e., spatial seismic ground motion considering all factors of spatial ground motion, have the highest values and present a random distribution according to the distance. While for the case of spatial seismic ground motion without considering local site effects, the generated displacements have lower values and a more regular distribution in space (Fig. 10).

We can see also, that the displacements generated in the case of spatial seismic ground motion without considering local site effects and those generated from the uniform seismic ground motion case are similar in terms of order of magnitude (size indication).

As it was noted above, the factors of spatial seismic ground motion are loss coherency, time delay effect and local site effect. Fig. 11 shows that local site effect can provide seismic ground motion higher than those generated considering only loss coherency and time delay effects.

In terms of seismic ground motion, it is clear that neglecting local site effect, i.e., considering only the loss coherency and time delay effects lead to an underestimation of the seismic loading that will be applied to the structure.

5.2 Structural dynamic analysis

Several dynamic analysis of the viaduct model are made using displacement time histories. The generated displacements are applied at the bottom of each viaduct support.

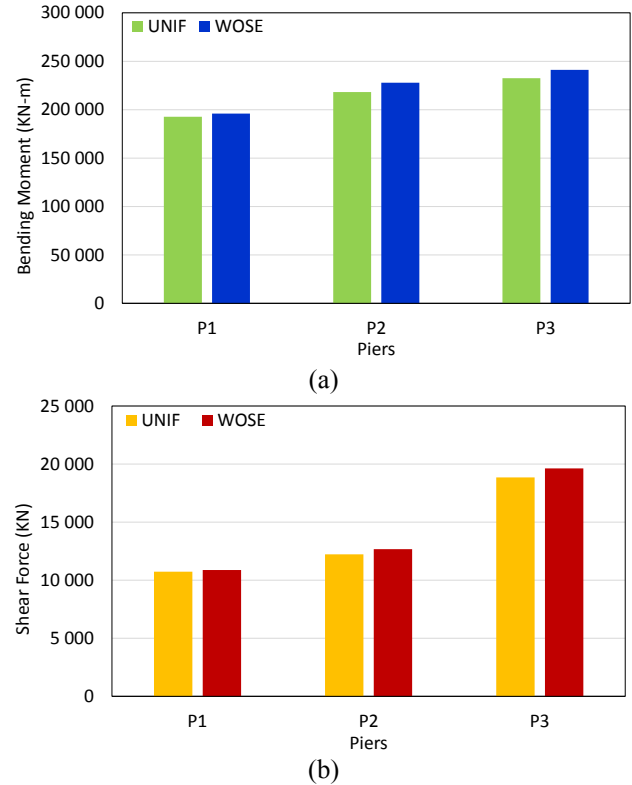


Fig. 13 Comparison of dynamic response of piers under spatial ground motion without considering site effect and uniform ground motion. (a) Maximum bending moment. (b) Maximum shear force

As explained above, four cases of ground motions were generated to be applied to viaduct structure. These four cases are: spatial seismic ground motion considering all factors of spatial ground motion (noted WSE: with site effect), spatial seismic ground motion without considering local site effect (noted WOSE: without site effect), spatial seismic ground motion with considering only local site effect and (noted SE Only: site effect) and uniform seismic ground motion (noted UNIF: Uniform).

The results of the structural dynamic analysis, subjected to the four cases of excitations are compared in terms of bending moment and shear force in piers. The maximum values of the bending moments and shear force obtained at each pier are illustrated in Figs. 13 to 16.

It is known that a uniform seismic ground motion consists to apply in the same time, an identical loading in acceleration or in displacement at all the supports of an extended structure.

At the first, the results of the dynamic analysis of the viaduct model under a spatial ground motion taking into account the effect of loss coherence and time delay (WOSE) are compared with those given by a uniform ground motion (UNIF). It is noted that the bending moments developed by a spatial ground motion without considering site effect are slightly higher than those given by a uniform seismic ground motion for the three piles of viaduct. This increase varies between 2% and 5% (Fig. 13(a)). The same observation is given for shear force at the three piles with the same variation rates (Fig. 13(b)).

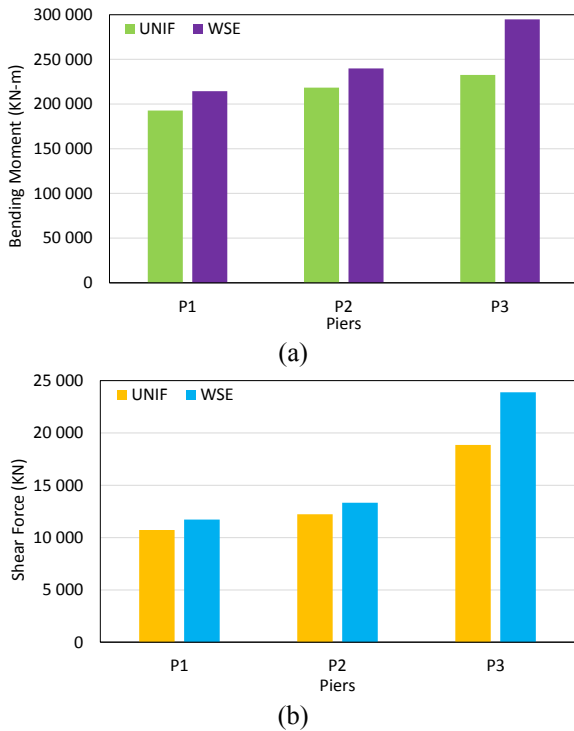


Fig. 14 Comparison of dynamic response of piers under spatial ground motion with considering site effect and uniform ground motion. (a) Maximum bending moment. (b) Maximum shear force

Secondly, internal forces provided by viaduct structure subjected to a spatial seismic ground motion taking into account all factors of the spatial variability of ground motion, namely loss coherency effect, time delay effect and site effect (WSE) are compared with those developed for uniform ground motion. Indeed, spatial seismic ground motion WSE gives bending moments greater than those developed by a uniform ground motion. The increase at the first and second piers (P1 and P2) is about 10%. For the third pier P3, a significant increase appears with a ratio of 22%. (Fig. 14(a)). The same variations were observed comparing shear force at the three piers P1, P2 and P3 (Fig. 14(b)).

The next phase consists at comparing the internal forces developed by viaduct structure under a spatial ground motion taking into account the effects of loss coherency and time delay (case WOSE), case of the major seismic codes approached by a simple formulation, and those given for a real seismic ground motion that takes all factors of spatial variability of seismic ground motion in particular site effect (case WSE). In Fig. 15, the bending moments of WSE case are greater than those developed by WOSE case for the three piers. The variation of bending moments and shear force is about 5% for the first pier P1 and 8% for the second pier P2. This ratio rises to 18% for the last pier P3 (Fig. 15(a)-(b)).

Finally, the results of dynamic analysis under spatial ground motion WOSE are compared with those given under spatial ground motion where only site effect was retained (SE only). In fact, the “SE only” case provide bending moments higher than those calculated from spatial ground

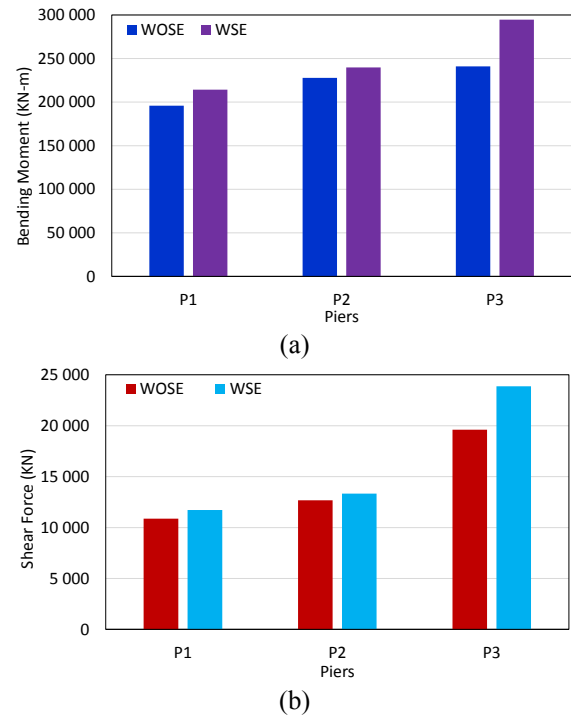


Fig. 15 Comparison of dynamic response of piers under spatial ground motion with and without considering site effect. (a) Maximum bending moment. (b) Maximum shear force

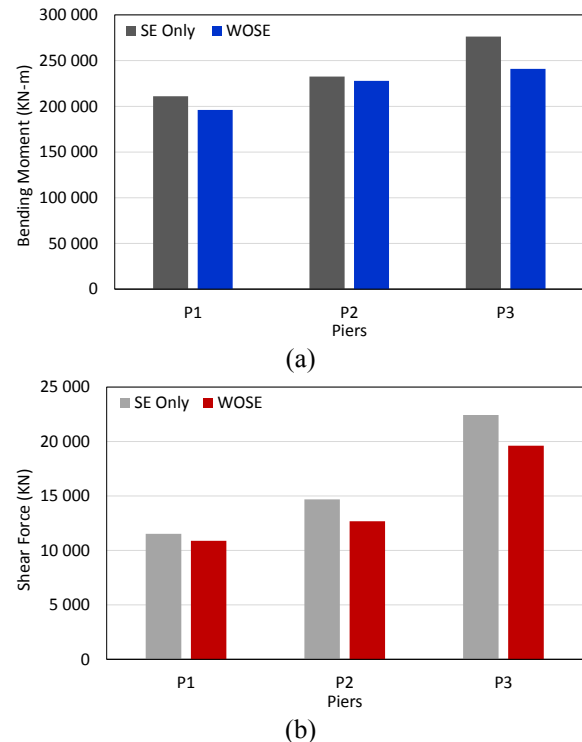


Fig. 16 Comparison of dynamic response of piers under spatial ground motion without considering site effect and that with considering only local site effect. (a) Maximum bending moment. (b) Maximum shear force

motion WOSE in particular for the third pier P3 with a variation ratio about 13%. While for the first pier P1, this

ratio became 7%. The variation of bending moments at second pier P2 is negligible (Fig. 16(a)). Comparing shear force, we found the same remarks. The variation is about 5% for pier P1 and 13% for piers P2 and P3 (Fig. 16(b)).

During a seismic analysis under a spatial variable ground motion, the dynamic response is very sensitive to the variations of the displacements imposed at the base.

In this case, it is evident that adopting a spatial seismic ground motion by considering only loss coherency and time delay effects leads to an underestimation of seismic demand.

8. Conclusions

A spatial seismic ground motion simulation model was developed. The proposed model takes into account all factors of spatial earthquake ground motion. Several spatial seismic ground motion are generated following the proposed model. These generated time history seismic ground motions are applied as seismic inputs to a curved viaduct.

Four dynamic analysis of the viaduct model are made according to seismic ground motion cases. WSE, WOSE, SE Only and UNIF. The internal forces of the structural dynamic analysis, subjected to the four cases of excitations are compared in terms of bending moments and shear force in piers.

Results of this study show that the dynamic analysis of viaduct under spatial seismic ground motion taking into account all factors of spatial ground motion, in particular, local site conditions leads to an increase of the seismic demand. The local site conditions can generate an amplification of seismic ground motion. Neglecting site effect, case of several studies, can lead to an underestimation of the internal forces developed by a structure.

References

- Adanur, S., Altunişik, A.C., Soyluk, K., Bayraktar, A. and Dumanoglu, A.A. (2016), "Multiple-support seismic response of Bosphorus Suspension Bridge for various random vibration methods", *Case Stud. Struct. Eng.*, **5**, 54-67. <https://doi.org/10.1016/j.csse.2016.04.001>.
- Beneldjouzi, M., Laouami, N. and Slimani, A. (2017), "Numerical and random simulation procedure for preliminary local site characterization and site factor assessing", *Earthq. Struct.*, **13**(1), 79-87. <https://doi.org/10.12989/eas.2017.13.1.079>.
- Benmansour, N. (2013), "Effet de la variabilité spatiale du mouvement sismique sur le comportement dynamique des ponts", Thèse de Doctorat, Université Abou Bekr Belkaid, Tlemcen, Algérie.
- Benmansour, N., Djafour, M., Bekkouche, A., Zendagui, D. and Benyacoub, A. (2012), "Seismic response evaluation of bridges under differential ground motion: a comparison with the new Algerian provisions", *Eur. J. Environ. Civil Eng.*, **16**(7), 863-881. <https://doi.org/10.1080/19648189.2012.681951>.
- Benmansour, N., Djafour, M., Zendagui, D. and Bekkouche, A. (2012), "Non linear dynamic analysis of bridge to spatially variable multiple support excitations", *9th International Conference on Urban Earthquake Engineering/ 4th Asia Conference on Earthquake Engineering*, Tokyo Institute of Technology, Tokyo, Japan.
- Bi, K. and Hao, H. (2012), "Modelling and simulation of spatially varying earthquake ground motions at sites with varying conditions", *Prob. Eng. Mech.*, **29**, 92-104. <https://doi.org/10.1016/j.probengmech.2011.09.002>.
- Bi, K., Hao, H. and Chouw, N. (2010), "Required separation distance between decks and at abutments of a bridge crossing a canyon site to avoid seismic pounding", *Earth. Eng. Struct. Dyn.*, **39**, 303-323. <https://doi.org/10.1002/eqe.943>.
- Bi, K., Hao, H. and Ren, W. (2010), "Response of a frame structure on a canyon site to spatially varying ground motions", *Struct. Eng. Mech.*, **36**(1), 111-127. <https://doi.org/10.12989/sem.2010.36.1.111>.
- Clough, R.W. and Penzien, J. (1993), *Dynamics of Structures*, McGraw Hill, New York.
- Deodatis, G. (1996), "Non-stationary stochastic vector processes: seismic ground motion applications", *Prob. Eng. Mech.*, **11**, 149-168. [https://doi.org/10.1016/0266-8920\(96\)00007-0](https://doi.org/10.1016/0266-8920(96)00007-0).
- Der Kiureghian, A. (1996), "A coherency model for spatially varying ground motions", *Earthq. Eng. Struct. Dyn.*, **25**(1), 99-111. [https://doi.org/10.1002/\(SICI\)1096-9845\(199601\)25:1<99::AID-EQE540>3.0.CO;2-C](https://doi.org/10.1002/(SICI)1096-9845(199601)25:1<99::AID-EQE540>3.0.CO;2-C).
- Derbal, R., Benmansour, N. and Djafour, M. (2017), "Influence de l'effet de site sur le comportement dynamique des ponts", *23^{ème} Congrès Français de Mécanique*, France, Lille, August-September.
- Derbal, R., Benmansour, N. and Djafour, M. (2018), "Impact of spatial variability of earthquake ground motion on seismic response of a railway bridge", *Int. J. Comput. Meth.*, **6**(5), 910-920.
- Dumanoglu, A.A. and Soyluk, K. (2003), "A stochastic analysis of long span structures subjected to spatially varying ground motions including the site-response effect", *Eng. Struct.*, **25**(10), 1301-1310. [https://doi.org/10.1016/S0141-0296\(03\)00080-4](https://doi.org/10.1016/S0141-0296(03)00080-4).
- Harichandran, R. and Vanmarcke, E. (1986), "Stochastic variation of earthquake ground motion in space and time", *J. Eng. Mech.*, **112**, 154-174. [https://doi.org/10.1061/\(ASCE\)0733-9399\(1986\)112:2\(154\)](https://doi.org/10.1061/(ASCE)0733-9399(1986)112:2(154)).
- Jennings, P.C., Housner, G.W. and Tsai, N.C. (1968), "Simulated earthquake motions", Report of Earthquake Engineering Research Laboratory, EERL-02, California Institute of Technology.
- Konakli, K. and Der Kiureghian, A. (2012), "Simulation of spatially varying ground motions including incoherence, wave-passage and differential site-response effects", *Earthq. Eng. Struct. Dyn.*, **41**(3), 495-513. <https://doi.org/10.1002/eqe.1141>.
- Miao, Y., Yao, E., Ruan, B. and Zhuang, H. (2018), "Seismic response of shield tunnel subjected to spatially varying earthquake", *Tunnel. Underg. Space Technol.*, **77**, 216-226. <https://doi.org/10.1016/j.tust.2018.04.006>.
- Safak, E. (1995), "Discrete-time analysis of seismic site amplification", *J. Eng. Mech.*, **121**(7), 801-809. [https://doi.org/10.1061/\(ASCE\)0733-9399\(1995\)121:7\(801\)](https://doi.org/10.1061/(ASCE)0733-9399(1995)121:7(801)).
- Shiravand, M.R. and Parvanehro, P. (2019), "Spatial variation of seismic ground motion effects on nonlinear responses of cable stayed bridges considering different soil types", *Soil Dyn. Earthq. Eng.*, **119**, 104-117. <https://doi.org/10.1016/j.soildyn.2019.01.002>.
- Tajimi H. (1960), "A statistical method of determining the maximum response of a building structure during an earthquake", *Proceeding of 2nd World Conference on Earthquake Engineering*, Tokyo, Japan, 781-796.
- Wolf, J.P. (1985), *Dynamic Soil-Structure Interaction*, Prentice Hall, Englewood Cliffs, NJ.
- Yao, E., Miao, Y., Wang, S. and Long, X. (2018), "Simulation of fully nonstationary spatially variable ground motions on a

- canyon site”, *Soil Dyn. Earthq. Eng.*, **115**, 198-204.
<https://doi.org/10.1016/j.soildyn.2018.08.030>.
- Zerva, A. (2009), “Spatial Variation of Seismic Ground Motions: Modeling and Engineering Applications” CRC Press, Group, Taylor & Francis.
- Zhang, D.Y., Liu, W., Xie, W.C. and Pandey, M.D. (2013), “Modeling of spatially correlated, site-reflected, and nonstationary ground motions compatible with response spectrum”, *Soil Dyn. Earthq. Eng.*, **5**, 21-32.
<https://doi.org/10.1016/j.soildyn.2013.08.002>.

AT